Enhancement of surface resistivity due to anisotropic Guinier-Preston zone scattering

1989 J. Phys.: Condens. Matter 1 8887

(http://iopscience.iop.org/0953-8984/1/45/014)

J. Phys.: Condens. Matter 1 (1989) 8887–8899. Printed in the UK

Enhancement of surface resistivity due to anisotropic Guinier–Preston zone scattering

I Nakamichi
Laboratory of Crystal Physics, Faculty of Science, Hiroshima University, Hiroshima 730, Japan

Received 8 November 1988, in final form 15 March 1989

Abstract. The residual electrical resistivity of dilute aluminium–silver foils with thicknesses of 30–1300 μm has been measured. The silver concentration is 0.01–0.1 at.%, and three heat treatments are used, referred to here as furnace cooling, air quenching and quenching followed by aging. The resistivities of foils show various features consistent with the presence of Guinier–Preston (GP) zones. A strong enhancement of surface resistivity ρ_s (= foil resistivity − bulk resistivity) is found in these foils: ρ_s increases with solute concentration and becomes about 4–5 times as large as that in the solid solution and in Fuchs–Sondheimer theory. The enhanced ρ_s decreases to about a half upon aging for 6 days at 350 K after quenching from 871 K. These results strongly suggest that anisotropy in GP zone scattering enhances ρ_s.

1. Introduction

There have been many studies of electrical conduction in thin metals, as reviewed by Larson (1971) and Bass (1972). However, in comparison with the direct effects of a surface, such as roughness, little is known of the effect of bulk scattering on surface resistivity. Here, the surface resistivity ρ_s in a thin metal is defined as

$$\rho_s = \rho - \rho_b \tag{1}$$

where ρ is the measured resistivity of the thin metal and ρ_b is the bulk resistivity; ρ_s contains the interaction term between surface and bulk scattering, namely that from impurities, phonons, etc. Theoretically, Bate *et al* (1963) have predicted that anisotropy in bulk scattering enhances ρ_s, but this has not been shown experimentally for a long time. However, a recent experiment by the present author has provided evidence supporting this prediction (Nakamichi and Kino 1988, referred to as NK2). That is, their dilute Al–Ag foils have shown much smaller ρ_s at 4.2 K than those of pure Al at low temperatures. In addition, ρ_s is in excellent agreement with Fuchs–Sondheimer (FS) theory based on the isotropic relaxation time (Fuchs 1938, Sondheimer 1952), in comparison with that in pure Al at low temperatures. Since Al–Ag solid solution has a nearly isotropic relaxation time at 4.2 K (Yonemitsu *et al* 1978, 1982, Sato *et al* 1978) in contrast to phonons at low temperatures, these results strongly suggest that anisotropy in bulk scattering enhances ρ_s and support Bate *et al*'s prediction.

In order to confirm this anisotropy enhancement mechanism experimentally, it is desirable to change the magnitude of anisotropy in the same alloy and to examine how

0953-8984/89/458887 + 13 $02.50

ρ_s changes. The Al–Ag alloy is known to have clusters called Guinier–Preston (GP) zones at higher concentrations. The GP zones have been shown to have a strongly anisotropic relaxation time by many theoretical calculations of the resistivity due to GP zones (Hillel 1970, Hillel *et al* 1975, 1977, Yonemitsu and Matsuda 1976, Edwards and Hillel 1977, Hillel and Edwards 1977, Guyot and Simon 1977, Luiggi *et al* 1980, Hillel and Rossiter 1981, Luiggi 1984). Therefore, anisotropic scattering due to GP zones is expected to enhance ρ_s in more concentrated Al–Ag alloys, in contrast to the case in solid solution. The detection of such enhancement will strongly support the anisotropy enhancement mechanism on ρ_s. Moreover, such detection would also provide evidence for Hillel *et al*'s theory, which predicts strong anisotropy in GP zone scattering. GP zones are well known to cause a resistivity anomaly during their growth, but the mechanism has not been settled yet, although it has long been studied both theoretically and experimentally since Mott's (1937) theory.

Thus, the previous resistivity measurements on Al–Ag foils have been extended to more concentrated foils, and silver concentrations and heat treatments have been varied to examine the effect of anisotropic scattering by GP zones on ρ_s. The results are discussed in connection with the previous results on Al–Ag solid solution and with FS theory, Bate *et al*'s theory and Hillel *et al*'s theory.

2. Experimental procedures

Specimens of Al–Ag polycrystal foils were prepared from zone-refined aluminium (Kino *et al* 1976) with bulk resistance ratio of 18 000 (referred to as ZR Al 1), doped with silver of purity 99.999% at concentrations of 0.0106, 0.0313 and 0.100 at.%. The concentrations were analysed by an activation analysis (Kino *et al* 1977) with relative accuracy better than 1%, using Al–0.100 at.% Ag as the standard. The foils have 30, 40, 50, 100, 200, 500 and 1300 μm thicknesses and 5 mm width, which are the same sizes as in NK2. Other details of specimen preparation have been described previously (NK2).

Seven foils with various thicknesses and the same silver concentration were annealed simultaneously at 823 K for 2 h in a vacuum of 1×10^{-4} Pa in a horizontal furnace, and were pulled out of the furnace into air at 423 K, midway through cooling. This heat treatment is referred to as air quenching. The first resistivity measurement was made. The foils were again annealed at 823 K for 2 h in the same way as above, but this time they were cooled in the furnace to room temperature. This is referred to as furnace cooling. Then, the second measurement was made. This furnace cooling introduces the possibility of forming small GP zones (Osono *et al* 1978), and has the advantage of giving exactly the same heat treatment to all the specimens in the furnace. In order to check the effect of surface change during the above heat treatments, foil surface layers a few micrometres thick were etched off with a chemical solution of $70H_3PO_4 + 25H_2SO_4 + 5HNO_3$ after the second measurement, and their resistivities were measured on Al–0.03 at.% Ag alloy.

In order to develop GP zones with oversaturated vacancies, quenching followed by aging was performed on pairs of thin and thick Al–0.1 at.% Ag foils, as follows. The foils are about 30 and 450 μm thick, and the thick one can be regarded approximately as a bulk specimen. The two foils were hung on a quartz frame and Al leads were spot-welded onto them. Before quenching, they were annealed at 823 K in the same way as above and were furnace-cooled. They were solution-treated for 30 min at 621 or 871 K in a vertical furnace, quenched from each temperature to 273 K by dropping them from

the furnace into distilled water directly beneath it, and then transferred into liquid nitrogen after washing them with methanol at 253 K. The transfer into liquid nitrogen took 6 s after the quench. Electrical Cu leads were spot-welded onto Al leads attached to the specimen foils in liquid nitrogen, by pulling out the ends of coiled Al leads into the air. A pair of foils quenched from 621 K were aged at 290 K in a stirred alcohol bath and further at 300 K in an oil bath. The other pair of foils quenched from the higher temperature of 871 K were aged in the alcohol bath at 300 K and further at a higher temperature of 350 ± 0.1 K for about 6 days in the horizontal furnace in a vacuum of 1×10^{-4} Pa, to develop GP zones more fully. This temperature was set 3 K below 353 K; GP zones in Al–0.1 at.% Ag begin to dissolve at 353 K and fully dissolve to solid solution at 373 K, according to Osono (1989).

The residual electrical resistivity of a foil with solute concentration c, $\rho(4.2, c)$, was evaluated from the measured resistances of the foil, $R(4.2, c)$ at 4.2 K and $R(300, c)$ at 300 K, by

$$\rho(4.2, c) = \rho(300, c)R(4.2, c)/R(300, c) \tag{2}$$

where $\rho(300, c)$ is the resistivity at 300 K for an alloy with solute concentration c. These electrical resistances were measured with an Otto-Wolff KDE 84 potentiometer having a sensitivity of 3 nV. The resistance $R(300, c)$ was measured in the oil bath regulated at 300 ± 0.01 K. The resistivity $\rho(300, c)$ was determined by the same method as described previously (NK2). The relative error of $\rho(4.2, c)$ was ±0.01%. Here $\rho(4.2, c)$ is simply called ρ.

3. Experimental results

The residual resistivity ρ of furnace-cooled and air-quenched specimens is plotted against $1/d_r$ for three alloys containing 0.01, 0.03 and 0.1 at.% Ag in figure 1, where d_r is the reduced thickness defined as

$$d_r = 2 \times (\text{cross section/perimeter}) \tag{3}$$

to take into account the limited foil width (Dingle 1950). Open symbols are for furnace-cooled specimens, closed symbols are for those air-quenched from 423 K and the symbols × are for those etched after furnace cooling. The numbers show the order of measurement on the same foils. All sets of data for each specimen lie on straight lines, showing a linear dependence of ρ on $1/d_r$. However, the slopes of these lines increase with solute concentration, in contrast to the previous result on more dilute alloys below 0.01 at.% Ag, where the slopes are almost independent of concentration (NK2). The etching off of surface layers causes almost no change to the slope for furnace-cooled foil data of Al–0.03 at.% Ag. The furnace-cooled specimens have smaller ρ, smaller slopes and smaller scatter of data than the air-quenched specimens, except for the most dilute alloy of 0.01 at.% Ag.

Variations in ρ of furnace-cooled foils during aging at 300 K are plotted against aging time for Al–0.1 at.% Ag alloy in figure 2. In spite of being furnace-cooled specimens, ρ of both foils with reduced thicknesses 30 and 455 μm increase with aging time, though very slowly.

The same foils as in figure 2 were quenched from 621 to 273 K after the above measurement, and aged at 290 K for 1×10^4 s and further at 300 K. The variations in ρ of these foils are plotted against aging time in figure 3, where the data at the aging time

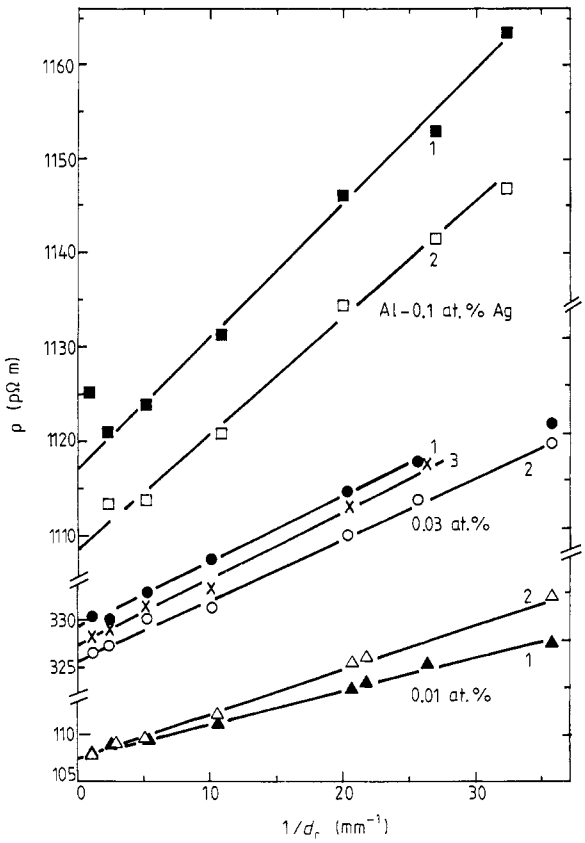

Figure 1. The residual resistivity ρ of Al–Ag foils plotted against the inverse of reduced thickness d_r for three silver concentrations. Open symbols, furnace-cooled foils; full symbols, foils air-quenched from 423 K; ×, foils etched after furnace cooling. The numbers show the order of measurement on the same foils.

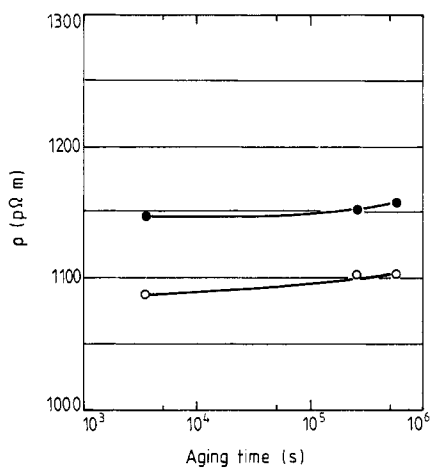

Figure 2. The variation of the residual resistivity ρ as a function of aging time at 300 K for Al–0.1 at.% Ag foils cooled in the furnace after annealing at 823 K. Reduced thickness: ●, 30 μm; ○, 455 μm.

of 6 s are those just after the quench. Both curves of thin and thick foils have maxima at about 500 s and the difference between them is about 50 pΩ m at that time. After passing through the maximum, ρ decreases very slowly in the thin foil but rapidly in the thick one. This size dependence of the decrease was recognised on other different thicknesses, omitted here.

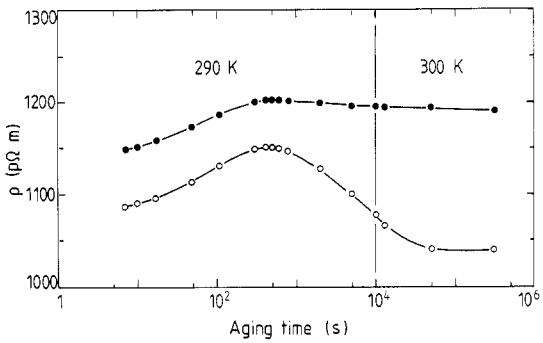

Figure 3. The variation of residual resistivity ρ as a function of aging time for Al–0.1 at.% Ag foils quenched from 621 K. The foils are the same as those in figure 2 and were aged at 290 K for 1×10^4 s and further at 300 K. Reduced thickness: ●, 30 μm; ○, 455 μm.

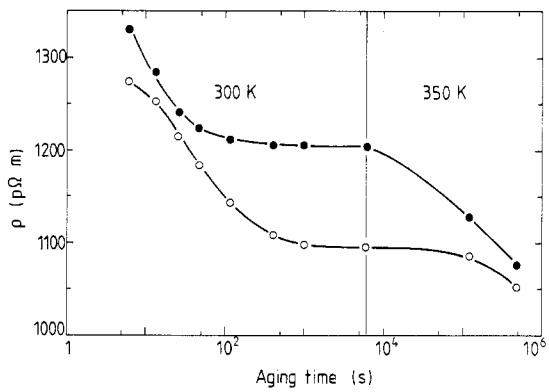

Figure 4. The variation of residual resistivity ρ as a function of aging time for Al–0.1 at.% Ag foils quenched from 871 K. They were aged at 300 K for 6×10^3 s and further at 350 K. Reduced thickness: ●, 31 μm; ○, 450 μm.

The ρ of Al–0.1 at.% Ag foils quenched from a higher temperature of 871 K are plotted against aging time in figure 4. These foils have nearly the same reduced thicknesses of 31 and 450 μm as above, and were aged at 300 K for 6×10^3 s and further at 350 K. The ρ show no maximum and decrease rapidly in the initial period of aging; the decrease stops around 10^2 and 10^3 s on the thin and thick foils, respectively, on aging at 300 K. However, ρ begin to decrease again rapidly in the thin foil, and then in the thick one upon aging at 350 K, the difference between the curves becoming a small value of 25 pΩ m after 4.9×10^5 s.

4. Analysis and discussion

4.1. ρ_s on furnace-cooled and air-quenched foils

Fuchs (1938) and Sondheimer (1952) derived the following equation for the electrical resistivity ρ of foils with thickness d, assuming isotropic scattering in metals,

$$\frac{\rho}{\rho_b} = \left[1 - \frac{3(1-p)}{2\kappa}\int_1^\infty \left(\frac{1}{t^3} - \frac{1}{t^5}\right)\frac{1 - e^{-\kappa t}}{1 - p\,e^{-\kappa t}}\,dt\right]^{-1} \tag{4}$$

where p is the specularity parameter, defined as the fraction of specular scattering at the

Table 1. The bulk quantities ρ_b, l_b and $\rho_b l_b$ determined by the fit of the experimental data to FS theory for Al–Ag alloys and zone-refined Al (ZR Al) at 4.2 K, and the solute contribution to ρ_b per unit concentration, $\Delta\rho_b/c$: $\Delta\rho_b$ is the difference of ρ_b between the alloy and ZR Al 1 used as the host metal; c is the silver concentration; and $\rho(300, c)$ is the resistivity at 300 K determined for the alloys.

Specimen	c (at.%)	ρ_b (pΩ m)	l_b (μm)	$\rho_b l_b$ (fΩ m^2)	$\Delta\rho_b/c$ (nΩ m/at.%)	$\rho(300, c)$ (nΩ m)
ZR Al 1		1.50				
ZR Al 2		2.00	340	0.680		
Al–Ag	0.00108	18.30*	39.9*	0.731*		
Al–Ag	0.00316	33.22*	23.8*	0.789*	10.0*	27.04
Al–Ag	0.0106	107.8*	6.94*	0.748*	10.0*	27.26
		107.8	9.74	1.05	10.0	
Al–Ag	0.0313	329.4*	4.68*	1.54*	10.5*	27.63
		325.5	4.49	1.46	10.4	
Al–Ag	0.100	1117*	2.71*	3.03*	11.2*	28.24
		1108	2.32	2.57	11.1	

* Values for the alloys air-quenched from 423 K.

surface, $\kappa = d/l_b$, and l_b and ρ_b are the electron mean free path and the bulk resistivity, respectively (FS theory). When $d_r > l_b/2$, a simple equation

$$\rho = \rho_b + 0.46(1 - p)\rho_b l_b/d_r \tag{5}$$

agrees with the above exact equation (4) (Kirkland and Chaplin 1971). The data shown in figure 1 are analysed with equation (5), where we take $p = 0$ (diffuse scattering) according to previous experimental results on Al (Nakamichi and Kino 1980). We can obtain the values of ρ_b and $\rho_b l_b$ from the intersections at $1/d_r = 0$ and the slopes of the lines in figure 1, respectively. The obtained values of ρ_b and l_b and the product $\rho_b l_b$ are listed in table 1, together with previous results (NK2) on more dilute Al–Ag alloys and zone-refined Al (referred to as ZR Al 2). Only for ZR Al 1 used as the host metal for alloys can the value of ρ_b be obtained from the measured resistivity of a foil with 500 μm thickness and equation (5), using the value of 0.68 fΩ m^2 as $\rho_b l_b$ for zone-refined Al. It should be noted that the value of $\rho_b l_b$ on Al–Ag is nearly constant at concentrations below 0.01 at.% Ag but increases rapidly with concentration above that level.

This rapid increase in $\rho_b l_b$ shown by the slope of the line in figure 1 can arise from either contamination during heat treatment or enhancement of surface resistivity ρ_s. If contamination were the cause, furnace cooling after air quenching should increase ρ more than air quenching, because contamination should increase ρ with the number of heat treatments. However, as seen in figure 1, furnace cooling decreases ρ and the slope of the lines for Al–0.03 and Al–0.1 at.% Ag alloys. Thus, contamination does not cause the increase in $\rho_b l_b$, although this shows that foil resistivity is very sensitive to this kind of heat treatment. As for ρ_s, we can obtain it from equation (1) with the measured resistivity and the values of ρ_b in table 1. The value of ρ_s is plotted against ρ_b for six foil thicknesses in figure 5. The figure also contains experimental data on more dilute Al–Ag and zone-refined Al obtained previously (NK2). The broken curves are the values calculated from FS theory. The calculation is performed by the same method as the previous one (Nakamichi and Kino 1980, NK2), where the values of $\rho_b l_b = 0.80$ fΩ m^2 and $p = 0$ are used. We see that ρ_s increases rapidly with concentration above

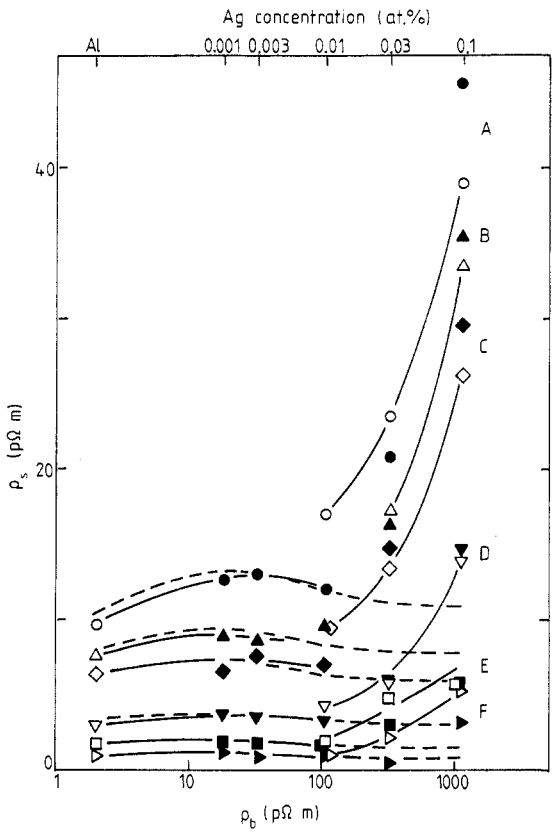

Figure 5. The surface resistivity ρ_s in Al and dilute Al–Ag alloys plotted against the bulk resistivity ρ_b for various thicknesses of foils. Reduced thickness: A, 28 μm; B, 39 μm; C, 50 μm; D, 97 μm; E, 189 μm; F, 470 μm. Open symbols, furnace-cooled foils; full symbols, foils air-quenched from 423 K. Broken curves are values calculated from FS theory with $\rho_b l_b = 0.80$ fΩ m^2 for $p = 0$. Full curves are to guide the reader's eyes for experimental values of air-quenched foils at concentrations below 0.01 at.% Ag, but above this, for those of furnace-cooled ones with less scatter in data. Data at concentrations below 0.01 at.% Ag are taken from our previous paper (NK2).

0.01 at.% Ag, and attains a large magnitude, which is about four times as large as that in alloys below 0.01 at.% Ag and that of FS theory. This is in contrast to the good agreement between FS theory and experiment on alloys below 0.01 at.% Ag, where the solute atoms are in the solid solution state. This enhancement of ρ_s is much larger than that due to phonon scattering in the temperature range 13–35 K, where ρ_s is enhanced by phonon scattering but is at most twice as large as that in Al–Ag solid solution (NK2).

This strong enhancement of ρ_s can be attributed to changes not in the surface layer but in the interior, because taking off the specimen surface layer of Al–0.03 at.% Ag foils does not change the slope of the line in figure 1. In fact, the solute contribution to ρ_b per unit concentration ($\Delta\rho_b/c$ in table 1) increases with concentration above 0.01 at.% Ag, where $\Delta\rho_b$ is the difference of ρ_b between the alloy and ZR Al 1. This indicates the formation of clusters in the alloys above 0.01 at.% Ag. This clustering phenomenon agrees with the solubility of Al–Ag alloy at 300 K, which is estimated to be around 0.01 at.%Ag by the extrapolation of data in Hansen and Anderko's (1958) book. Moreover, the constant value of $\Delta\rho_b/c$ (10.0 nΩ m/at.% below 0.01 at.% Ag in table 1) agrees well with the value of 10 nΩ m/at.% for solid solution given by Fickett (1971). The $\Delta\rho_b/c$ of 11.1 nΩ m/at.% for furnace-cooled Al–0.1 at.% Ag also agrees well with 11.2 nΩ m/at.% obtained for furnace-cooled Al–0.1 at.% Ag by Kawata and Kino (1975), who analysed the solute concentration with atomic absorption spectroscopy. Therefore, we can attribute the observed enhancement of ρ_s to clusters in these alloys.

4.2. ρ_s on quenched and aged foils

Osono *et al* (1978) have shown by a resistometric method that GP zones are formed even in furnace-cooled Al–1 at.% Ag, and their recent extension has shown that the same occurs in Al–0.1 at.% Ag also (Osono 1989). Thus, we have tried to develop GP zones and measure ρ_s, to examine whether the enhancement of ρ_s is caused by GP zones, as follows.

Since quenching from high temperatures accelerates the growth of GP zones during aging with quenched-in vacancies (Turnbull *et al* 1960), this heat treatment is adopted on Al–0.1 at.% Ag foils. The GP zones are known to show certain features on such heat treatment. First, it is well known that the resistivity increases with growth of GP zones during aging and then decreases with their further growth, showing a maximum in age-hardening alloys such as Al–Ag, Al–Cu and Al–Zn (Turnbull *et al* 1960, Kelly and Nicholson 1963, Osamura *et al* 1973). We see such a maximum in figure 3. Both its amplitude and the time to reach it show order-of-magnitude agreement with other experimental results on Al–1.4 at.% Ag (Turnbull *et al* 1960) and on Al–0.5 at.% Ag (Yonemitsu 1972), which have similar quenching and aging temperatures. Secondly, GP zones in Al–Ag are known, by diffraction measurements, to form during quenching because they grow rapidly in this alloy (Walker and Guinier 1953, Ernst and Haasen 1987). Figure 3 shows that ρ just after the quench is already larger than that for a solid solution of this alloy (1002 pΩ m) and suggests that clusters are formed during the quench in the present case also. The value of 1002 pΩ m is estimated as (10.0 nΩ m/at.%) $\times$ (0.100 at.%) + 1.5 pΩ m from table 1, and the above increase in ρ is much larger than that due to quenched-in vacancies: 10 pΩ m for this quench (Furukawa *et al* 1976). Thirdly, a recent resistivity and small-angle x-ray measurement on Al–4 and Al–10 wt.% Zn foils (Ohta *et al* 1986) has shown the following: after the resistivity maximum, thin foils have a smaller decrease in their resistivity and smaller size of GP zones than thick foils, when the quenching temperature is not too high (<650 K). That is, the growth of GP zones stops earlier in the thin foil, probably because the quenched-in vacancies can reach the surface much earlier in the thin foil and annihilate there, ceasing to act as carriers of solute atoms. This phenomenon is also seen in figure 3: ρ decreases much more slowly in the thin foil than in the thick one after the resistivity maximum. These agreements on features strongly suggest that GP zones are formed by this heat treatment.

As described above, after the resistivity maximum, the zone size is different between thin and thick foils, and thus we cannot get ρ_s from a simple difference of ρ between thin and thick foils. However, both foils have maxima at 500 s for this heat treatment, as seen in figure 3. This suggests that the differences of zone size and zone number between the two foils are negligible during aging up to 500 s (at least at 500 s). Thus, we can take the difference of ρ between the two foils as ρ_s for the thin foil at least at 500 s, regarding the thick one as bulk, and we can do this approximately up to 500 s. We see the following from figures 2 and 3 for the same foils: (i) the difference of ρ between thin and thick foils is 50 pΩ m at 500 s in figure 3, and is 4–5 times as large as that in Al–Ag solid solution (see figure 5); (ii) this difference does not change much during aging up to 500 s; and (iii) it is nearly the same as that in the furnace-cooled foils (figures 2 and 3). In addition, (iv) the resistivities in the furnace-cooled foils correspond to those in the initial aging period in the quenched foils, with respect to their magnitude and increasing behaviour with time (figures 2 and 3). From these, we can draw the following conclusions on Al–0.1 at.% Ag, for foils quenched from 621 K and aged at 290 K, and for furnace-cooled foils. First, it is strongly suggested that GP zones cause enhancement of ρ_s in quenched

foils, from point (i) combined with the suggestion in the preceding paragraph. Secondly, the enhancement does not change much during the early period of aging (point (ii)). Thirdly, the clusters in the furnace-cooled foils are suggested to correspond to those in the initial growth stage in the quenched foils, from point (iv); it is noted that precipitates decrease ρ in general and do not show the increase of ρ with time seen in the furnace-cooled foils, without GP zones in the initial growth stage. Lastly, these and point (iii) lead to the suggestion that GP zones cause enhancement of ρ_s in the furnace-cooled foils, the same as in the quenched ones.

In order to avoid the above stopping of zone growth in thin foils and to examine whether ρ_s changes when zones develop more fully, quenching was carried out at higher temperature, as shown in figure 4. The ρ already pass through the maximum at the beginning of aging and decrease rapidly. This phenomenon has often been seen in Al–Ag when quenched from fairly high temperatures, and is attributed to their rapid clustering (Turnbull *et al* 1960, Kelly and Nicholson 1963). However, the decrease stops again at 10^2 s in the thin foil and at 10^3 s in the thick one. This means that clusters again stop their growth earlier in the thin foil. Thus, the aging temperature was raised up to 350 K from 6000 s to give more vacancies and sufficient solute mobility to develop zones. This temperature is much lower than the transition temperature of the GP zone state; it is known by diffraction measurements that GP zones are in a state called the η-GP zone below about 440 K and they change to the ε-GP zone with lower Ag content above 440 K (Bauer and Gerold 1962, Gerold *et al* 1964, Osamura *et al* 1986). In addition, a recent high-resolution electron microscopy measurement has shown that η-GP zones continue to increase their size in Al–1 at.% Ag on aging up to 700 h at 413 K after quenching from 748 K (Ernst and Haasen 1987). As expected, we see that ρ begin to decrease again from 6000 s by raising the temperature up to 350 K in figure 4. Although γ' precipitates are known to grow after GP zone growth in Al–Ag and to decrease ρ, this occurrence seems to be observed only at higher aging temperatures above 430 K and at higher solute concentrations above several atomic per cent (Kelly and Nicholson 1963, Osamura *et al* 1986). Moreover, if this precipitation were the cause, it should occur in both foils and decrease both resistivities simultaneously, because the foils were simultaneously given the same heat treatment. However, in contrast to the large decrease in ρ in the thin foil, that in the thick one is very small at first on aging at 350 K. Thus, the decrease in ρ must mean not γ' precipitation but growth of GP zones. Probably, since GP zones remained at the earlier growth stage in the thin foil and thus had more driving force for growth, they must have grown faster than those in the thick foil when they could begin to grow again. Thus, it is expected that the zone size in the thin foil becomes near to that in the thick one by this further growth. Again, therefore, we take the difference of ρ between both foils as ρ_s. The difference is 25 pΩ m in the final period of aging, 4.9×10^5 s (6 days). This value is about a half of ρ_s at 500 s in the early period of aging in figure 3. This means that ρ_s decreases upon this heat treatment. This suggests that the enhancement of ρ_s becomes small when GP zones become rather large.

4.3. Enhancement of ρ_s and anisotropic GP zone scattering

Classical theories of the size effect have assumed isotropic bulk scattering both in FS theory for foils and in Dingle's (1950) theory for wires. However, Bate *et al* (1963) have shown that anisotropy in l_b increases both ρ_s and the apparent value of $\rho_b l_b$ by a factor

$\langle l_b^2\rangle/\langle l_b\rangle^2$ for a polycrystalline wire, when the diameter of the wire and the grain size are much greater than l_b, using kinetic theory (Chambers 1950). Here,

$$\langle l_b\rangle = \int l_b(\boldsymbol{k}_F)\,\mathrm{d}S_F/S_F \tag{6}$$

and

$$\langle l_b^2\rangle = \int l_b^2(\boldsymbol{k}_F)\,\mathrm{d}S_F/S_F \tag{7}$$

where the integral is taken over the Fermi surface, and $\boldsymbol{k}_F$ and S_F are the electron wavevector on the Fermi surface and the Fermi surface area, respectively. The enhancement factor $\langle l_b^2\rangle/\langle l_b\rangle^2$ is larger than 1 when l_b is anisotropic. Similar enhancement by anisotropic scattering is expected for foils also. That is, similarly to Bate *et al*'s equation for wires, equation (5) for foils is expected to have the form

$$\rho = \rho_b + (\langle l_b^2\rangle/\langle l_b\rangle^2)0.46(1-p)\rho_b\langle l_b\rangle/d_r \tag{8}$$

when the thickness and grain size are much greater than l_b. This condition is satisfied in the present alloys with concentration above 0.01 at.% Ag, as seen in table 1, because the thinnest foil in the present work is 30 μm thick and grain sizes are usually near to the foil thickness. The second term in equation (8) corresponds to ρ_s, and the factor $\langle l_b^2\rangle/\langle l_b\rangle^2$ enhances ρ_s when l_b is anisotropic. In this case, the enhancement factor increases the slopes of lines such as those in figure 1, and the value of $\rho_b l_b$ obtained from the slope becomes larger than that in the case of isotropic bulk scattering.

In the present experiment, we can obtain the enhancement factor by dividing the values of $\rho_b l_b$ in table 1 by 7.6 fΩ m^2, which is the value of $\rho_b l_b$ for Al–Ag solid solution with a nearly isotropic relaxation time (NK2). The enhancement factor obtained is plotted against $\Delta\rho_b/c$ for three alloys containing 0.01, 0.03 and 0.1 at.% Ag in figure 6. The specimens are furnace-cooled (open symbols) or air-quenched from 423 K (full symbols). The lines are values for the solid solution. We see that the enhancement factor increases monotonically and rapidly from 1 to 4 with $\Delta\rho_b/c$, almost irrespective of heat treatment.

As for the anisotropy in GP zone scattering, Hillel's (1970) theory for the resistivity due to GP zones predicts the following: in his calculation with the pseudopotential method, the square of the structure factor in the matrix element of the potential for GP zones has a form similar to the expression for the intensity of x-rays scattered from a regular array of lattice points in a crystal; the structure factor is maximised (Bragg peak) by the same condition as the Bragg law in diffraction theory. The Bragg peak in $\boldsymbol{k}$-space becomes high and narrow with the GP zone radius. This leads to the following predictions: (i) The relaxation time is nearly isotropic when the GP zone is small because the Bragg peak is low and broad. (ii) When the GP zone radius becomes larger than the inverse of the mean separation of the Fermi surface from the Brillouin zone boundary, the Bragg peak begins to localise around the Brillouin zone boundary and causes Bragg scattering; the relaxation time is now strongly $\boldsymbol{k}$-dependent (i.e. anisotropic). (iii) When GP zones grow fairly large, the Bragg peak becomes very narrow and the Bragg scattering becomes a vanishing small fraction of the Fermi surface, decreasing the contribution to ρ (Hillel *et al* 1975, Hillel and Rossiter 1981).

Uniting these with the anisotropy enhancement mechanism on ρ_s, we can compare these predictions with the observed features of enhancement, in connection with the zone growth below. First, in the initial growth stage, the fraction of zones with anisotropic

scattering is predicted to increase rapidly with average zone size from points (i) and (ii), because zones have a size distribution (Ernst and Haasen 1987). This is suggested to be consistent with the rapid increase in enhancement factor with $\Delta\rho_b/c$ in the furnace-cooled or air-quenched foils seen in figure 6, because zones can develop both with solute

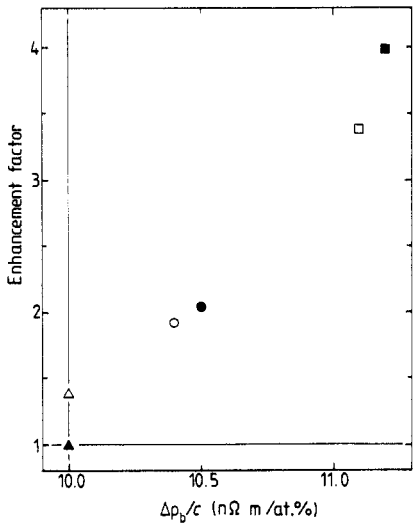

Figure 6. The enhancement factor plotted against the solute contribution to ρ_b per unit concentration, $\Delta\rho_b/c$. Triangles, Al–0.01 at.% Ag; circles, Al–0.03 at.% Ag; squares, Al–0.1 at.% Ag; open symbols, furnace-cooled foils; full symbols, foils air-quenched from 423 K.

concentration (Bauer and Gerold 1961, Osamura *et al* 1973) and by aging after air quenching, and increase $\Delta\rho_b/c$ in the initial growth stage; or zone numbers might increase with solute concentration, bringing about an increase in fraction of anisotropic scattering, and partly cause this phenomenon. Secondly, in their following growth stage, most zones are predicted to have anisotropic scattering from point (ii). This probably corresponds to the nearly constant value of strongly enhanced ρ_s during the initial aging after quenching from 621 K, as described in § 4.2 (figure 3). Thirdly, for large zones, the enhancement factor $\langle l_b^2\rangle/\langle l_b\rangle^2$ integrated over the Fermi surface is expected to be small from point (iii). This is suggested to be consistent with the observation of a decrease in ρ_s on aging at 350 K for 6 days, because this aging is suggested to develop zones in § 4.2 (figure 4). In addition, since Yonemitsu and Matsuda (1976) have calculated the relaxation time for GP zones in Al–Ag alloy and shown their result along a line on the Fermi surface, we can approximately estimate the magnitude of the enhancement factor $\langle l_b^2\rangle/\langle l_b\rangle^2$ with it. This estimation gives a value of 2 for the enhancement factor of the zone, and has order-of-magnitude agreement with experiment.

5. Summary and conclusions

The residual resistivity ρ has been measured on thin foils of dilute Al–Ag alloys (0.01–0.1 at.% Ag) subjected to a variety of heat treatments. The foils show an increase in the solute contribution to ρ_b per unit concentration ($\Delta\rho_b/c$) at concentrations above 0.01 at.% Ag. A strong enhancement of surface resistivity ρ_s is found in these foils:

(i) ρ_s in furnace-cooled or air-quenched foils increases rapidly with $\Delta\rho_b/c$ and with solute concentration, and becomes about 4–5 times as large as that in solid solution and FS theory; this is 2–3 times as large as that enhanced by anisotropic phonon scattering; (ii) the ρ_s enhanced in Al–0.1 at.% Ag does not change much during the initial period of aging at 290 K after quenching from 621 K, and is nearly the same as that in furnace-cooled foils; and (iii) it decreases to about a half upon aging for 6 days at 350 K after quenching from 871 K. Although observations with the diffraction method have not been made, ρ show various features consistent with the presence of a GP zone and its growth, and the features of enhanced ρ_s can be explained with the theoretical predictions from the following two mechanisms: (i) anisotropy in bulk scattering enhances ρ_s, and (ii) GP zones have strongly anisotropic scattering arising from Bragg scattering which depends on their size. These suggest that the size effect measurement gives useful knowledge to clarify the mechanism of GP zone scattering and will be more advanced when combined with diffraction measurements.

Acknowledgments

I would like to thank Professor T Kino for much advice and encouragement. I wish to acknowledge Dr E Hashimoto for the activation analysis of alloys; Dr H Osono for helpful discussion of GP zone formation, and Professor K Yonemitsu for offering the original figure of relaxation time for GP zones.

References

Bass J 1972 *Adv. Phys.* **21** 431–604
Bate R T, Martin B and Hille P F 1963 *Phys. Rev.* **131** 1482–8
Bauer R and Gerold V 1961 *Z. Metallk.* **52** 671–6
—— 1962 *Acta Metall.* **10** 637–45
Chambers R G 1950 *Proc. R. Soc.* A **202** 378–94
Dingle R G 1950 *Proc. R. Soc.* A **201** 545–60
Edwards J T and Hillel A J 1977 *Phil. Mag.* **35** 1221–9
Ernst F and Haasen P 1987 *Phys. Status Solidi* a **104** 403–16
Fickett F R 1970 *Cryogenics* **11** 349–67
Fuchs K 1938 *Proc. Camb. Phil. Soc.* **34** 100–8
Furukawa K, Takamura J, Kuwana N, Tahara R and Abe M 1976 *J. Phys. Soc. Japan* **41** 1584–92
Gerold V, Auer H and Merz W 1964 *Adv. X-ray Anal.* **7** 1–13
Guyot P and Simon J P 1977 *Scr. Metall.* **11** 751
Hansen M and Anderko K 1958 *Constitution of Binary Alloys* (New York: McGraw-Hill)
Hillel A J 1970 *Acta Metall.* **18** 253–9
Hillel A J and Edwards J T 1977 *Phil. Mag.* **35** 1231
Hillel A J, Edwards J T and Wilkes P 1975 *Phil. Mag.* **32** 189–209
—— 1977 *Phil. Mag.* **35** 829–30
Hillel A J and Rossiter P L 1981 *Phil. Mag.* B **44** 383–8
Kawata S and Kino T 1975 *J. Phys. Soc. Japan* **39** 684–91
Kelly A and Nicholson R B 1963 *Progress in Material Science* vol 10 ed B Chalmers (Oxford: Pergamon) pp 149–391
Kino T, Hashimoto E, Kamigaki N, Kiso Y and Matsushita R 1977 *Trans. Japan. Inst. Met.* **18** 305–12
Kino T, Kamigaki H, Yamasaki H, Kawai J, Deguchi Y and Nakamichi I 1976 *Trans. Japan. Inst. Met.* **17** 645–8
Kirkland L R and Chaplin R L 1971 *J. Appl. Phys.* **42** 3054–7
Larson D C 1971 *Phys. Thin Films* **6** 81–149

Luiggi N 1984 *J. Phys. F: Met. Phys.* **14** 2601–12
Luiggi N, Simon J P and Guyot P 1980 *J. Phys. F: Met. Phys.* **10** 865–72
Mott N F 1937 *J. Inst. Met.* **60** 267
Nakamichi I and Kino T 1980 *J. Phys. Soc. Japan* **49** 1350–7
—— 1988 *J. Phys. F: Met. Phys.* **18** 2421–8
Ohta M, Kanadani T, Yamada M and Sakakibara A 1986 *J. Japan. Inst. Met.* **50** 887–92
Osamura K, Hiraoka Y and Murakami Y 1973 *Phil. Mag.* **28** 809–10
Osamura K, Nakamura T, Kobayashi A, Hashizume T and Sakurai T 1986 *Acta Metall.* **34** 1563–70
Osono H 1989 in preparation
Osono H, Kawata S, Endo T and Kino T 1978 *Trans. Japan. Inst. Met.* **19** 69–76
Sato H, Babauchi T and Yonemitsu K 1978 *Phys. Status Solidi* b **89** 571–6
Sondheimer E H 1952 *Adv. Phys.* **1** 1–42
Turnbull D, Rosenbaum H S and Treaftis H N 1960 *Acta Metall.* **8** 277–95
Walker C B and Guinier A 1953 *Acta Metall.* **1** 568–77
Yonemitsu K 1972 *Phys. Status Solidi* a **13** 325–31
Yonemitsu K and Matsuda T 1976 *Phys. Status Solidi* a **36** 791–8
Yonemitsu K, Sato H, Fujita Y and Sakamoto I 1982 *J. Phys. F: Met. Phys.* **12** 2653–61
Yonemitsu K, Takano K and Matsuda T 1978 *Phys. Status Solidi* b **88** 273–82